Chemistry–A European Journal

Communication
doi.org/10.1002/chem.202001389

Macrocyclic Chemistry

Active Metal Template Synthesis and Characterization of a Nanohoop [*c*2]Daisy Chain Rotaxane

Jeff M. Van Raden, Nanette N. Jarenwattananon, Lev N. Zakharov, and Ramesh Jasti*[a]

Abstract: Molecules and materials that demonstrate large amplitude responses to minor changes in their local environment play an important role in the development of new forms of nanotechnology. Molecular daisy chains are a type of a mechanically interlocked molecule that are particularly sensitive to such changes in which, in the presence of certain stimuli, the molecular linkage enables muscle-like movement between a reduced-length contracted form and an increased-length expanded form. To date, all reported syntheses of molecular daisy chains are accomplished via passive-template methods, resulting in a majority of structures being switchable only through the addition of an exogenous stimuli such as metal ions or changes in pH. Here, we describe a new approach to these structural motifs that exploits a multi-component active-metal template synthesis to mechanically interlock two pi-rich nanohoop macrocycles into a molecular daisy chain that undergoes large conformational changes using thermal energy.

When downsizing machinery to the nanoscale, the ability to mimic design principles of macroscopic machinery becomes increasingly difficult. For example, at the molecular scale, objects undergo sporadic, unplanned movements due to Brownian motion.[1] However, in the macroscopic world, objects are not strongly affected by such random motion and as a result, the planned, orchestrated movement of numerous components in a machine is readily accomplished. Developing strategies to overcome hurdles such as this have therefore emerged as a key focus point for generating new types nanotechnology. Mechanically interlocked molecules such as rotaxanes and catenanes represent a unique class of molecules that display properties of motion common to both micro and macroscopic objects,[2] suggesting structures of this form can provide a platform to merge macroscopic principles with molecular scale systems. Importantly, the specific connectivity of the mechanical linkage dictates what type of motion can be harnessed which, in principle, can be leveraged by a variety of actuation mechanisms such as pH, metal-coordination, and redox chemistry.[2]

With a name originating from the similarity between daisy chain garlands, a less explored, yet particularly powerful mechanically interlocked molecular architecture are cyclic and linear daisy chain rotaxanes.[3] The simplest cyclic form can be understood as a [*c*2]daisy chain (Figure 1 a), where *c* refers to cyclic and 2 represents the number of mechanically interlocked components. A prized feature of [*c*2]daisy chains is the ability to actuate these motifs between extended or contracted states (Figure 1 a). This results in muscle-like motion, which can give rise to large changes in molecular dimensions[3a] and shape.[3c] Thus, when viewed as components for investigating nanoscale motion through macroscopic actuation, these structures represent especially fascinating targets. To date, a majority of the reported daisy chain architectures are actuated through light,[3d] pH,[3d–g] electrochemical,[3h,i] and metal-coordination-based mechanisms,[3a,c,j] with thermally actuated systems being relatively rare.[3d] This likely stems from the typical method of preparation, in which interactions such as metal-coordination and radical–radical pairing template the formation of the desired daisy chain.[3] These passive-template approaches result in a mechanically interlocked structure where the employed host–guest interaction “lives on” in the final product, resulting in strong intercomponent binding energies.

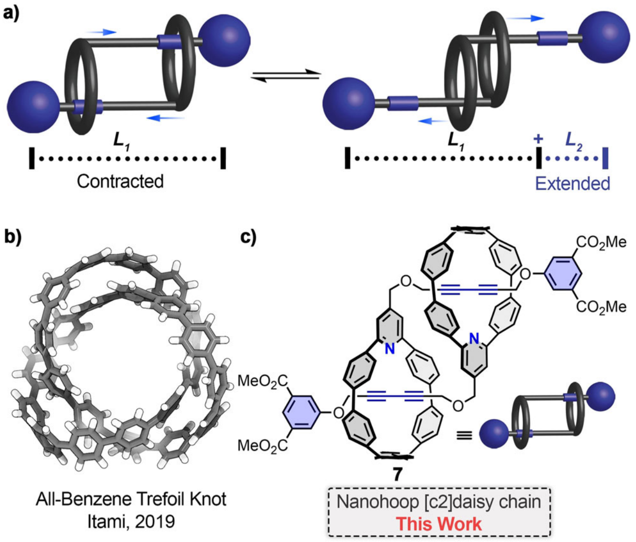

Figure 1. a) Cartoon illustration showing a contracted and extended state of a [c2]daisy chain rotaxane. b) All-benzene molecular trefoil knot prepared by Itami. c) Nanohoop [c2]daisy chain prepared in this work.

---

[a] Dr. J. M. Van Raden, Dr. N. N. Jarenwattananon, Dr. L. N. Zakharov, Prof. R. Jasti
University of Oregon
Eugene, Oregon OR-97403 (USA)
E-mail: rjasti@uoregon.edu

Supporting information and the ORCID identification number(s) for the author(s) of this article can be found under: https://doi.org/10.1002/chem.202001389.

While the mechanical bond allows each component to translate, rotate, or contract relative to each other, it is the molecular composition of the underlying components that determine properties such as rate of shuttling, strength of contraction or mechanism of actuation. Structurally distinct from typical interlocked molecules, pi-rich molecular nanocarbons[4] such as cycloparaphenylenes or "nanohoops"[4] have emerged as interesting platforms for modulating and studying motion at the nanoscale. For example, a recent report by Itami et al. showed that a fully conjugated all-benzene trefoil knot displays rapid vortex-like motion at temperatures far below room temperature.[4l] Additionally, work by Isobe et al. has demonstrated that nanohoop macrocycles can provide a pathway to ratchet-free solid-state motion.[4m] Recently, we demonstrated a synthetic method to thread sp-hybridized fragments (diynes) through small-diameter pi-rich macrocycles using an active metal Cadiot–Chodkiewicz template (AT-CC) synthesis.[4n] Fundamentally different from a passive-template strategy, this AT-CC approach provides a mechanically interlocked molecule that contains no complimentary interaction between macrocycle and thread component in the final interlocked molecule.[5] As a result, weaker interaction energies between thread and macrocycle are observed.[5c] Encouraged by this prospect and the emerging properties of nanocarbons,[4] we report here the formation of a [*c*2]daisy chain rotaxane bearing two carbon-rich nanohoop macrocycles (Figure 1 c) that have been mechanically interlocked via two sp-hybridized diyne threads. The key mechanical bonds are forged via AT-CC reaction, providing the final structure in good yield. We show that this structure can rapidly contract and expand via thermal energy—a rare consequence of both structural composition and the AT-CC method of preparation.

Our work first began by investigating the feasibility of forming a [*c*2]daisy chain structure via an AT-CC reaction. We opted to expand on our recent work with 2,6-pyridine-embedded nanohoop macrocycles with the understanding that an AT-CC would likely allow for the formation of the desired structure. Accordingly, we began by first preparing a new functionalized nanohoop macrocycle containing an alkyl-linked terminal acetylene (Figure 2). To avoid introducing chirality into the nanohoop macrocycle, we targeted the *meta*-pyridine ring as the key point for functionalization. The synthesis began (Figure 2) by first preparing diboronate **1** and pyridine derivative **2** via literature procedures.[4n] Leveraging our previous synthetic strategy, we found that macrocycle **3** was readily accessed in 70% under dilute Suzuki–Miyaura conditions with **1** and **2**. Macrocycle **3** was then deprotected with tetrabutylammonium fluoride (TBAF) followed by reductive aromatization with H_2SnCl_4 to give the corresponding benzylic alcohol **4** in 61% over two steps. Conversion to the alkyne-functionalized macrocycle was accomplished via deprotonation with NaH in the presence of excess propargyl bromide in THF, giving the target macrocycle **5** in excellent yield.

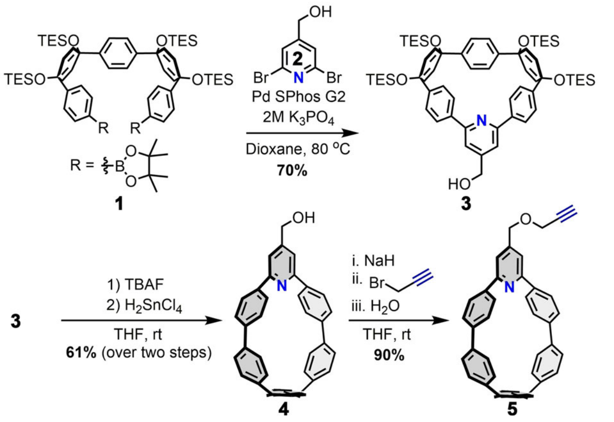

Figure 2. Synthetic strategy used to access terminal alkyne functionalized nanohoop **5**.

It should be noted that the formation of [*cn*]daisy chain structures requires *n* ($n > 1$) mechanical bonds to be formed, where *n* represents the number of units, that is, bonds formed, that comprise the final structure. While this has been observed in multi-component active metal template syntheses of catenanes[5d] as well in a related molecular knot,[5f] it has not been reported for the targeted daisy chain architecture. Accordingly, with **5** in hand, we then proceeded to explore the formation of the desired [*c*2]daisy chain via an AT-CC reaction (Figure 3 a). We first subjected **5** to our previously reported[4n] AT-CC conditions (toluene, 80 °C, K_2CO_3, $[Cu(MeCN)_4]PF_6$) with 3,5-diester-functionalized bromo-alkyne **6** (Figure 3) under dilute (5 mM) conditions, however, after purification, we observed a minor amount of cross-coupled unthreaded product along with sig-

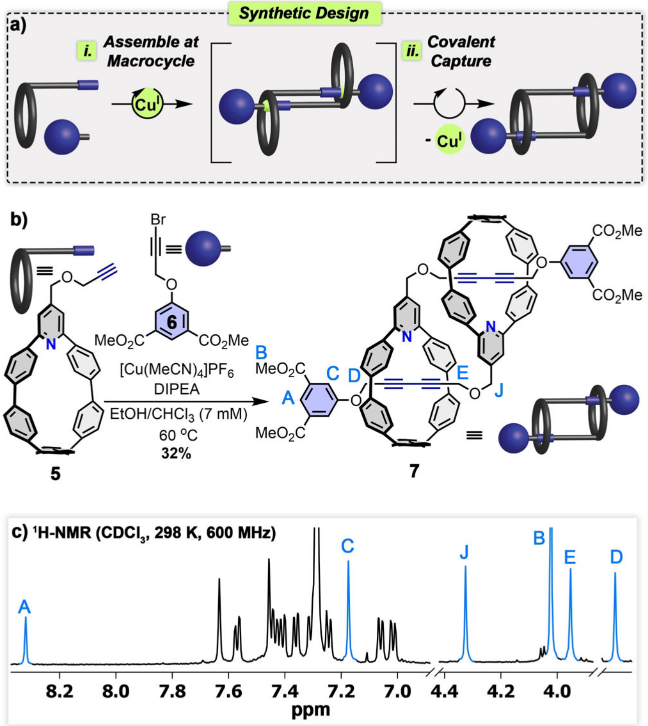

Figure 3. a) Cartoon representation illustrating the targeted synthetic approach toward **7**. b) Conditions used to form [*c*2]daisy chain rotaxane **7**. c) Partial ^{1}H-NMR spectrum of **7** ($CDCl_3$, 298 K, 600 MHz) showing assignment of thread protons H_{A-J}.

nificant amounts of unreacted starting materials. On closer inspection of the crude reaction mixture via ^{1}H NMR spectroscopy, we observed a small amount of an unidentified third product that we anticipated was the desired [*c*2]daisy chain. Isolation of this product revealed a relatively simple ^{1}H NMR spectrum (Figure 3 c) with several proton resonances appearing noticeably upfield (for example, resonance H_D)—evidence that suggested an interlocked molecule (see Supporting Information for all spectral data). Mass spectrometry of this product revealed an *m*/*z* that corresponded to two macrocyclic units (*m*/*z* = 1542.4724), allowing us to tentatively assign the structure to that of **7** (Figure 3 a). Intrigued by this small formation of **7**, we then screened various conditions in an effort to selectively prepare this product. We found that when the reaction was run under dilute conditions (7 mM) at 60 °C using (*N*,*N*-diisopropylethylamine) DIPEA as base and using a chloroform:ethanol (1:1) solvent system,[5d] the desired product **7** could be isolated in 32 % yield via chromatography. This is rather impressive given the demanding nature of the product—four separate molecular components must assemble together followed by the formation of two mechanical bonds. Thus, the formation of **7** further demonstrates the ability of the AT approach to act in multi-component synthesis.

With a sufficient quantity (ca. 20 mg) of **7** in hand, we next turned to single-crystal X-ray crystallography (SXRC) to confirm the identity of **7**, where we found that suitable crystals for diffraction could be grown via vapor diffusion of pentane into a concentrated solution **7** in THF. Accordingly, as revealed by SXRC (Figure 4), **7** is indeed an interlocked structure comprised of two units of macrocycle **7**, that is, a [*c*2]daisy chain. Unlike typical [*c*2]daisy chains, **7** is unusually small due to the macrocycles used in the AT preparation. Additionally, **7** is comprised of all sp^{2}-hybridized macrocyclic components, making it an overall very rigid system, a feature which was also reflected in a general lack of solubility in most solvents. Intrigued by the formation of **7**, we then investigated the geometrical features observed in the solid-state structure (Figure 4). As can be seen, the macrocyclic fragment is located over the ether-linkage between the diyne and stopper moiety with a distance of 3.34 Å between the nitrogen of the macrocycle and oxygen atom of the thread unit being observed (Figure 4 c and 4 d). Notably, a short contact of 3.03 Å was observed (Figure 4 c) which, in combination with the upfield resonance of H_D (Figure 3 c), suggests that C–H···pi interactions may be responsible for the preferred location of the nanohoop along the thread. Additionally, various short contacts between the hydrogen atoms of the methyl ester moiety were found, ranging between 2.44 and 2.90 Å from the methyl group to adjacent macrocycle (Figure 4 c and 4d). Taken together, these distances highlight the highly crowded environment within the macrocyclic pocket as well confirm a contracted, rather than expanded, solid-state conformation of **7**.

Upon isolation of **7**, we observed strong emission (Figure 5 a) with a measured emission maximum centered at 517 nm. It is well known that the parent hydrocarbon cycloparaphenylenes ([*n*]CPPs) possess bright fluorescent features and red-shifting emissions with decreasing macrocycle size.[4d] As the diameter is reduced, the fluorescence is no longer observed where a CPP comprised of six aryl rings (i.e. [6]CPP) is non emissive-a con-sequence of both strain and orbital symmetry.[6a] We recently found that the inclusion of *meta*-substituted aryl rings breaks orbital symmetry resulting in bright fluorescence from smaller macrocycles[6b] which provides a rationale for the observed emission of **7**. This was also observed in our previously reported rotaxanes bearing macrocycles of similar size.[4n] Additionally, we found that the quantum of yield of **7** ($\Phi = 0.15$) was nearly identical to that of our previously reported [2]rotaxanes, suggesting that the daisy chain architecture does not reduce the emission behavior. Lastly, in the absorption spectrum of **7** (Figure 5 a), two main absorptions were observed at approximately 330 and 420 nm, which is

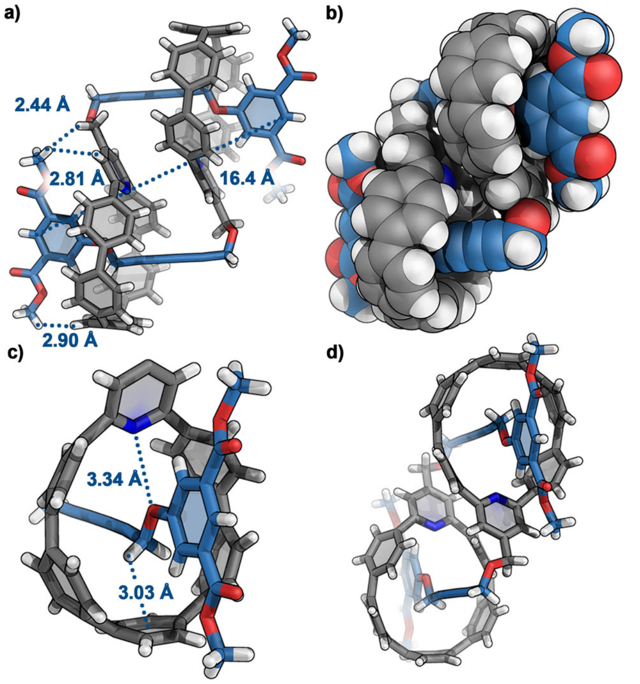

Figure 4. Solid-state X-ray structure of **7**. a) Space-fill representation of solid-state structure of **7**. b) Stick representation of **7** showing selected distances. c) and d) Ball and stick representations at two different angles showing selected distances observed within macrocyclic cavity and between ester moiety. For clarity, all hydrogen atoms are coloured white, carbons grey or blue oxygen atoms red, and nitrogen atoms blue. Solvent has been omitted. Blue carbons represent thread and stopper components of **7**.

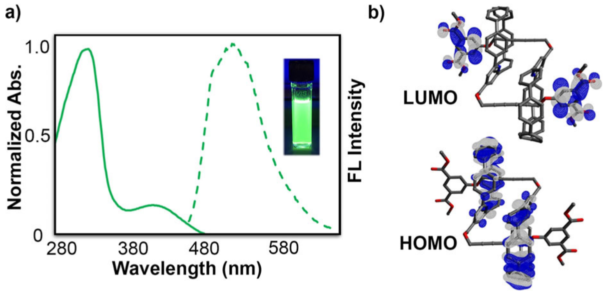

Figure 5. a) Absorption and emission spectra of **7** in dichloromethane. b) DFT calculated frontier molecular orbitals of **7**.

consistent with our previous report. Of note, DFT calculations show a spatial separation of the frontier molecular orbitals (Figure 5 b). While not investigated here, the emerging interest in nanohoop-based polymers[7a] as well as recent reports of mechanically interlocked fluorescent sensors[7b,c] suggests that interlocking nanohoop fluorophores into daisy chain architectures could serve as excellent starting point for the development of polymeric sensing materials.

In the presence of certain stimuli such as metals or protons, [*c*2]daisy chains can often be switched between either a contracted or expanded muscle-like state.[3] The actuation mechanism is highly dependent on the passive templating method used to prepare the structure. In contrast to most daisy chain structures, **7** has no complimentary interactions between the macrocycle and thread component due to the usage of an AT-CC method. It has been shown that this results in weak intercomponent binding energies which can allow for less common stimuli to actuate mechanical motion.[5c] Encouraged by this observation as well as related work by Takata et al.,[8] we targeted thermal energy as potential source to actuate **7**. To investigate this, we first carried out variable temperature (VT) ^{1}H NMR on **7** over a temperature range of −60 to 50 °C (Figure 6). We found that the resonance belonging to (See Figure 3 for assignments) H_D shifts upfield to nearly 1.3 ppm from 3.0 ppm, indicating stronger shielding at lower temperatures. On the other hand, resonances belonging to H_J and H_E are shifted downfield by nearly 1.0 ppm each, demonstrating an overall deshielding at lower temperatures. The effect of increased shielding of H_D and decreased shielding of H_J and H_E on lowering temperature suggests that as the temperature decreases, the macrocycle of **7** begins to reside pre-dominantly over the proton H_D. Taken further, this suggests that at lower temperatures, the conformation of **7** begins to adopt that of a contracted form whereas on heating, the macrocycle begin to participate in rapid shuttling over protons H_J, H_E, and H_D. This demonstrates that on the NMR timescale, fast muscle-like expansion and contraction is taking place and the macrocycle position, that is, daisy chain state, can be modulated by a decrease in temperature.

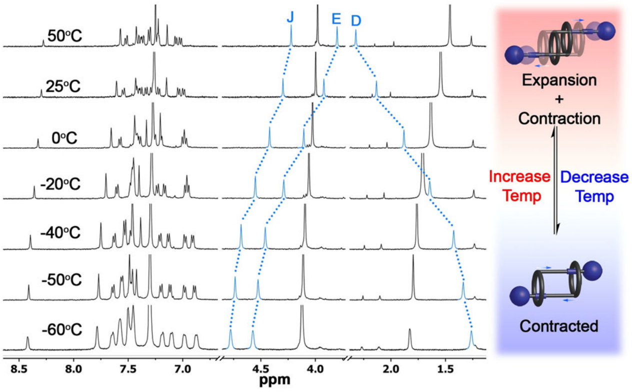

Figure 6. VT ^{1}H-NMR spectrum of **7** from −60 °C to 50 °C ($CDCl_3$ at 500 MHz). Cartoon illustrations on the right depict the observed motion occurring over the measured temperature range.

To further confirm the location of the macrocycle at various temperatures, we then probed these dynamics via VT selective 1D ROESY on resonance H_B (Figure 3 for assignment). At 25 °C two ROE signals between H_J and H_K are observed, suggesting that the ester moiety is close in proximity with both the benzylic proton (H_J) and pyridyl ring of the macrocycle. On heating the same sample to 50 °C, ROE signals between these resonances were still observed, but were significantly attenuated (Figure 6, right) suggesting a larger distance between each moiety at elevated temperature. This data supports the notion that at lower temperature, the macrocyclic ring resides near the stopper moiety, that is, a contracted form. It should be noted that temperature changes would be expected to impact the motion of nearly any molecular object, however, a direct consequence of the mechanical linkage in systems such as **7** is that the reduced motion of each bond at lower temperatures ultimately orchestrates a large amplitude change in molecular geometry, that is, contraction or extension (Figure 7). Taken together, these data illustrate that actuation of **7** can be achieved in an additive-free manner via thermal changes which we attribute directly to the lack of complimentary interactions between macrocycle and thread-a feature inherent the AT-CC method of preparation.

In conclusion, our work here provides the first example of an usual type of fluorescent, nanohoop [*c*2]daisy chain formed without an inherent interaction between each fragment—a structure which appears to be accessible only through at active template approach. While the lack of interaction between each component renders typical stimuli-induced expansion or contraction strategies unamenable, we show that this structure's conformation can be tuned via temperature which may allow for operation under a wider range of environmental conditions. Additionally, based on DFT calculations, we find that the frontier molecular orbitals are located between thread and macrocycle. Specifically, the HOMO is localized over the macrocycle while the LUMO is localized over the stopper moieties. We expect that by increasing the thread length, the dis-

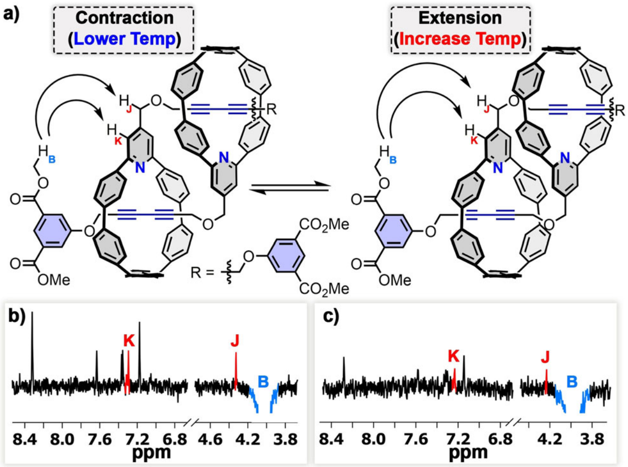

Figure 7. a) Cartoon illustration showing two different conformations of each macrocycle relative to the thread component. Detected 1D selective ROE signals observed on excitation of H_B at b) 25 °C and c) 50 °C.

tance between these groups can be altered via temperature changes which may allow for modulation of the emission. Additionally, given that a variety of active template reactions as well as macrocycle compositions are now known, more common stimuli-induced strategies such as metal-coordination can likely be leveraged through, for example, as AT copper(I)-catalyzed azide-alkyne cycloaddition reaction. This work ultimately highlights a new approach to link small carbon nanostructures with mechanical bonds—a strategy and concept that we expect will provide new momentum in the emerging area of supramolecular carbon nanoscience.

Acknowledgements

Financial support was provided by the National Science Foundation (NSF) (CHE-1808791 and CHE-1800586), the Camille and Henry Dreyfus Foundation. Additionally, we acknowledge the Murdock Charitable Trust (Grant #SR-2017297) for the acquisition of the single crystal X-ray diffractometer).

Conflict of interest

The authors declare no conflict of interest.

Keywords: active-template reactions · cycloparaphenylenes · macrocycle · mechanical bond · mechanically interlocked molecule

[1] a) S. Erbas-Cakmak, D. Leigh, C. T. Mcternan, A. L. Nussbaumer, *Chem. Rev.* **2015**, *115*, 10081 – 10206; b) F. Lancia, A. Ryabchun, N. Katsonis, *Nat Rev Chem* **2019**, *3*, 536 – 551; c) S. Kassem, T. van Leeuwen, A. S. Lubbe, M. R. Wilson, B. L. Feringa, D. A. Leigh, *Chem. Soc. Rev.* **2017**, *46*, 2592 – 2621.

[2] a) C. J. Bruns, J. F. Stoddart, *The Nature of the Mechanical Bond: From Molecules to Machines*; Wiley-VCH, Weinheim, **2016**; b) M. Dumartin, M. C. Lipke, J. F. Stoddart, *J. Am. Chem. Soc.* **2019**, *141*, 18308 – 18317; c) Y. Qiu, L. Zhang, C. Pezzato, Y. Feng, W. Li, M. T. Nguyen, C. Cheng, D. Shen, Q.-H. Guo, Y. Shi, K. Cai, F. M. Alsubaie, R. D. Astumian, J. F. Stoddart, *J. Am. Chem. Soc.* **2019**, *141*, 17472 – 17476.

[3] a) M. C. Jiménez, C. Dietrich-Buchecker, J. Sauvage, *Angew. Chem. Int. Ed.* **2000**, *39*, 3284 – 3287; *Angew. Chem.* **2000**, *112*, 3422 – 3425; b) J. Rotzler, M. Mayor, *Chem. Soc. Rev.* **2013**, *42*, 44 – 62; c) J. Chang, S. Tseng, C. Lai, Y. Liu, S. Peng, S. Chiu, *Nat. Chem.* **2017**, *9*, 128 – 134; d) R. E. Dawson, S. F. Lincoln, C. J. Easton, *Chem. Commun.* **2008**, 3980 – 3982; e) A. Wolf, A. J. Cid, E. Moulin, F. Niess, G. Du, A. Goujon, E. Busseron, A. Ruff, S. Ludwigs, N. Giuseppone, *Eur. J. Org. Chem.* **2019**, 3421 – 3432; f) Q. Zhang, S. Rao, T. Xie, X. Li, D. Qu, Y. Long, H. Tian, *Chem.* **2018**, *4*, 2670 – 2684; g) J. Wu, K. Leung, D. Benitez, J. Han, S. Cantrill, L. Fang, J. F. Stoddart, *Angew. Chem. Int. Ed.* **2008**, *47*, 7470 – 7474; *Angew. Chem.* **2008**, *120*, 7580 – 7584; h) C. J. Bruns, J. Li, M. Frasconi, S. T. Schneebeli, J. Lehl, H. J. De Rouville, S. L. Stupp, G. A. Voth, J. F. Stoddart, *Angew. Chem. Int. Ed.* **2014**, *53*, 1953 – 1958; *Angew. Chem.* **2014**, *126*, 1984 – 1989; i) C. J. Bruns, M. Frasconi, J. Lehl, K. J. Hartlieb, S. T. Schneebeli, C. Cheng, S. L. Stupp, J. F. Stoddart, *J. Am. Chem. Soc.* **2014**, *136*, 4714 – 4723; j) J. Collin, C. Dietrich-Buchecker, P. Gavina, M. C. Jimenez-Molero, J. Sauvage, *Acc. Chem. Res.* **2001**, *34*, 477 – 487.

[4] a) J. M. Van Raden, R. Jasti, *Science* **2019**, *365*, 216 – 217; b) R. Jasti, J. Bhattacharjee, J. B. Neaton, C. R. Bertozzi, *J. Am. Chem. Soc.* **2008**, *130*, 17646 – 17647; c) M. R. Golder, R. Jasti, *Acc. Chem. Res.* **2015**, *48*, 557 – 566; d) E. R. Darzi, R. Jasti, *Chem. Soc. Rev.* **2015**, *44*, 6401 – 6410; e) S. E. Lewis, *Chem. Soc. Rev.* **2015**, *44*, 2221 – 2304; f) M. Majewski, M. Stępień, *Angew. Chem. Int. Ed.* **2019**, *58*, 86 – 116; *Angew. Chem.* **2019**, *131*, 90 – 122; g) T. Iwamoto, Y. Watanabe, Y. Sakamoto, T. Suzuki, S. Yamago, *J. Am. Chem. Soc.* **2011**, *133*, 8354 – 8361; h) E. J. Leonhardt, R. Jasti, *Nat. Rev. Chem.* **2019**, *3*, 672 – 686; i) Y. Xu, R. Kaur, B. Wang, M. B. Minameyer, S. Gsanger, B. Meyer, T. Drewello, D. M. Guldi, M. von Delius, *J. Am. Chem. Soc.* **2018**, *140*, 13413 – 13420; j) Y.-Y. Fan, D. Chen, Z. Huang, J. Zhu, C. Tung, L. Wu, H. Cong, *Nat. Commun.* **2018**, 3037; k) P. Bäuerle, M. Ammann, M. Wilde, G. Götz, A. Rang, C. A. Schalley, *Angew. Chem. Int. Ed.* **2007**, *46*, 363 – 368; *Angew. Chem.* **2007**, *119*, 367 – 372; l) Y. Segawa, M. Kuwayama, Y. Hijikata, M. Fushimi, T. Nishihara, J. Pirillo, J. Shirasaki, N. Kubota, K. Itami, *Science* **2019**, *365*, 272 – 276; m) T. Matsuno, Y. Nakai, S. Sota, Y. Maniwa, H. Isobe, *Nat. Commun.* **2018**, *9*, 1907; n) J. M. Van Raden, B. M. White, L. N. Zakharov, R. Jasti, *Angew. Chem. Int. Ed.* **2019**, *58*, 7341 – 7345; *Angew. Chem.* **2019**, *131*, 7419 – 7423.

[5] a) V. Aucagne, K. D. Hanni, D. A. Leigh, P. J. Lusby, D. B. Walker, *J. Am. Chem. Soc.* **2006**, *128*, 2186 – 2187; b) M. Denis, S. M. Goldup, *Nat. Rev. Chem.* **2017**, *1*, 61; c) J. Berná, S. M. Goldup, A.-L. Lee, D. A. Leigh, M. D. Symes, G. Teobaldi, F. Zerbetto, *Angew. Chem. Int. Ed.* **2008**, *47*, 4392 – 4396; *Angew. Chem.* **2008**, *120*, 4464 – 4468; d) J. E. M. Lewis, F. Modiom, S. M. Goldup, *J. Am. Chem. Soc.* **2018**, *140*, 4787 – 4791; e) L. D. Movsisyan, M. Franz, F. Hamper, A. K. Thompson, R. R. Tykwinski, H. L. Anderson, *J. Am. Chem. Soc.* **2016**, *138*, 1366 – 1376; f) P. E. Barran, H. L. Cole, S. M. Goldup, D. A. Leigh, P. R. McGonigal, M. D. Symes, J. Wu, M. Zengerle, *Angew. Chem. Int. Ed.* **2011**, *50*, 12280 – 12284; *Angew. Chem.* **2011**, *123*, 12488 – 12492.

[6] a) L. Adamska, L. Nayyar, H. Chen, A. K. Swan, N. Oldani, S. Fernandex-Alberti, M. R. Golder, R. Jasti, S. K. Doorn, S. Tretiak, *Nano Lett.* **2014**, *14*, 6539 – 6546; b) T. C. Lovell, C. E. Colwell, L. N. Zakharov, R. Jasti, *Chem. Sci.* **2019**, *10*, 3786 – 3790.

[7] a) Q. Huang, G. Zhuang, M. Zhang, J. Wang, S. Wang, Y. Wu, S. Yang, P. Du, *J. Am. Chem. Soc.* **2019**, *141*, 18938 – 18943; b) Y. Sagara, M. Karman, E. Verde-Sesto, K. Matsuo, Y. Kim, N. Tamaoki, C. Weder, *J. Am. Chem. Soc.* **2018**, *140*, 1584 – 1587; c) Y. Sagara, M. Karman, A. Seki, M. Pannipara, N. Tamaoki, C. Weder, *ACS Cent. Sci.* **2019**, *5*, 874 – 881.

[8] K. Nakazono, T. Takata, *Chem. Eur. J.* **2010**, *16*, 13783 – 13794.

[9] CCDC 1977872 contain the supplementary crystallographic data for this paper. These data are provided free of charge by the joint Cambridge Crystallographic Data Centre and Fachinformationszentrum Karlsruhe Access Structures service www.ccdc.cam.ac.uk/structures..

Manuscript received: March 20, 2020
Accepted manuscript online: March 23, 2020
Version of record online: ■■ ■■, 0000

COMMUNICATION

Macrocyclic Chemistry

*J. M. Van Raden, N. N. Jarenwattananon, L. N. Zakharov, R. Jasti**

■■ – ■■

Active Metal Template Synthesis and Characterization of a Nanohoop [c2]Daisy Chain Rotaxane

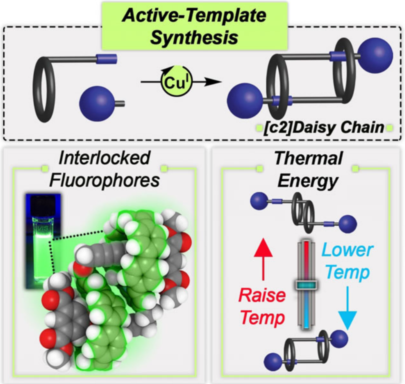

Molecular muscle: The synthesis and characterization of a fluorescent, small, pi-rich [c2]daisy chain is described. The synthesis is accomplished using a multicomponent Cu^{I}-catalysed active-template Cadiot–Chodkiewicz reaction, ultimately assembling four molecular components into a single mechanically interlocked architecture. Through variable temperature NMR, the motion of this structure is then described.